Materials Physics and Mechanics 42 (2019) 637-645 Received: March 26, 2019

PANTOGRAPHIC METAMATERIALS: A VIEW TOWARDS APPLICATIONS

Francesco dell'Isola[1,2], Ivan Giorgio[2], Luca Placidi[2,3], Mario Spagnuolo[2*], Patrice Peyre[4], Corinne Dupuy[4], Justin Dirrenberger[4], Marek Pawlikowski[5], Leonid Igumnov[1]

[1]Research Institute for Mechanics, National Research Lobachevsky State University of Nizhni Novgorod

[2]International Research Center M&MoCS, Università dell'Aquila

[3]Engineering Faculty, International Telematic University Uninettuno Roma

[4]PIMM, UMR 8006 CNRS- Arts et Métiers Paris-Tech, 75013 Paris, France

[5]Institute of Mechanics and Printing, Warsaw University of Technology, Warsaw, Poland

*e-mail: mario.spagnuolo.memocs@gmail.com

Abstract. The purpose of this article is to show the basic characteristics of the so-called pantographic metamaterial. Here we underline how the microstructure provides some exotic properties and, in principle, implies the second gradient nature of this type of metamaterial. Thanks to the development of additive manufacturing technology (especially in the field of metallurgy) we are now able to produce real samples and carry out experimental measurements to validate the proposed models. In this article we show some new experimental tests, obtained by considering pantographic structures printed in stainless steel. Numerical simulations are briefly shown to show the validity of the theoretical model developed to describe the pantographic metamaterial.

Keywords: pantographic metamaterials, second gradient theory, multi-scale models, homogenization

1. Introduction

It has been shown that, if the microstructure is complex enough, the resulting homogenized continuous model cannot be always framed in classic continuum mechanics [1-5]. Of particular interest in this family is the so-called pantographic material [6-9].

In this article we want to show how the basic deformation properties of pantographic structures depend only on their geometry, allowing us to talk about a new class of metamaterials. Clearly, the range of measured forces will depend on the material that constitutes the structure, but the constituent equations remain the same and we only need to modify the parameters to adapt them to the experimental measures. This peculiarity is typical of metamaterials and can be obtained through a procedure of homogenization, as described in [10-12].

http://dx.doi.org/10.18720/MPM.4252019_17

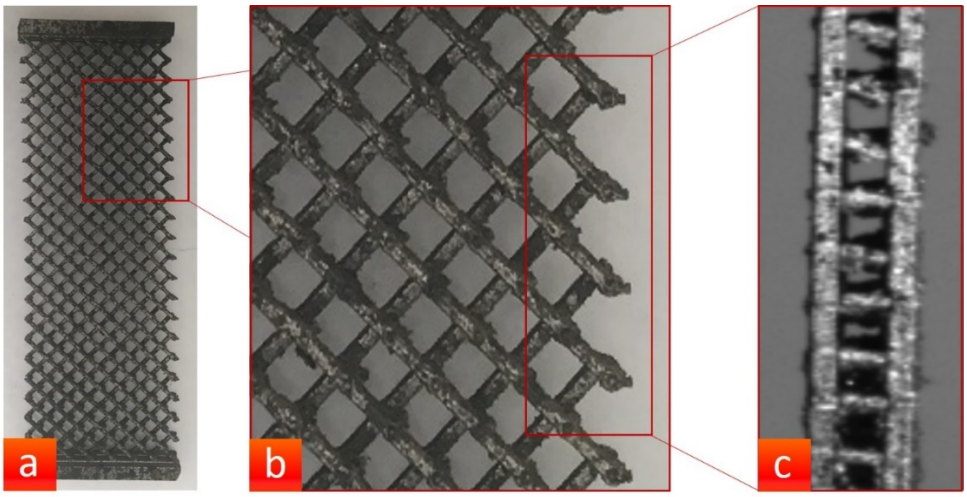

Fig. 1. A inox printed pantographic structure (a) and some particulars: the two families of fibers (b) interconnect in correspondence of some pivots (c).
We thank Prof. F. Hild and Dr. X. Pinelli for image (c)

It has been shown by Germain [13-14], Mindlin et al. [15-17], Toupin [18] and Sedov [19] how the presence of a microstructure can be described from a macroscopic point of view by introducing a second gradient (or strain gradient, as it was first called) term in the energy of the microstructured material.The pantographic structure to which we will refer corresponds to a real rectangular sample printed in 3D (see Fig. 1) consisting of a planar grid formed by two families of continuous fibers that intersect orthogonally and connect to each other in nodes that we call pivots (pivots do not interrupt the continuity of the fibers). Each fibre belonging to one of the two arrays is connected by the pivots to the fibres belonging to the other array. The real pivots are cylinders, whose torsion is a priori not negligible.

2. Second gradient homogenized model

In [8] it has been shown how to obtain a macroscopic second gradient continuum model by means of a process of homogenization (which specifically consists in performing a procedure of identification of the energy of macro-deformation, i.e. a macroscopic Lagrangian density (line or surface) of energy of deformation, in terms of the constituent parameters that appear in the postulated expressions of the energies of micro-deformation) of a postulated micro-model. If we assume a 2D continuum whose reference configuration is given by a rectangular domain $\Omega = [0, L_1] \times [0, L_2] \subset \mathbb{R}^2$ (for example, in Fig. 1 L_1 and L_2 represent the lengths of the sides of the ideal rectangle containing the pantographic structure) and assuming planar motion, the current configuration of Ω is described by the planar macro-placement.
$\boldsymbol{\chi}: \Omega \longrightarrow \mathbb{R}^2$.

In [8] it is proven that the continuum energy of a pantographic structure can be written as

$$\mathcal{U}(\boldsymbol{\chi}(\cdot)) = \int_\Omega \sum_\alpha \frac{\mathbb{K}_e}{2} (\|\boldsymbol{FD}_\alpha\| - 1)^2 \, d\Omega + \int_\Omega \sum_\alpha \frac{\mathbb{K}_b}{2} \left[\frac{\nabla \boldsymbol{F}|\boldsymbol{D}_\alpha \otimes \boldsymbol{D}_\alpha \cdot \nabla \boldsymbol{F}|\boldsymbol{D}_\alpha \otimes \boldsymbol{D}_\alpha}{\|\boldsymbol{FD}_\alpha\|^2} - \left(\frac{\boldsymbol{FD}_\alpha}{\|\boldsymbol{FD}_\alpha\|} \cdot \frac{\nabla \boldsymbol{F}|\boldsymbol{D}_\alpha \otimes \boldsymbol{D}_\alpha}{\|\boldsymbol{FD}_\alpha\|} \right)^2 \right] d\Omega \quad (1) + \int_\Omega \sum_\alpha \frac{\mathbb{K}_p}{2} \left| arccos \left(\frac{\boldsymbol{FD}_1}{\|\boldsymbol{FD}_1\|} \cdot \frac{\boldsymbol{FD}_2}{\|\boldsymbol{FD}_2\|} \right) - \frac{\pi}{2} \right|^\gamma d\Omega,$$

where $\boldsymbol{F} = \nabla \boldsymbol{\chi}$ and $(\nabla \boldsymbol{F}|\boldsymbol{D}_\alpha \otimes \boldsymbol{D}_\alpha)^\beta = \boldsymbol{F}^\beta_{\alpha,\alpha} = \boldsymbol{\chi}^\beta_{,\alpha\alpha}$ and no sum over repeated α is intended; the γ exponent characterizes the torsional deformation of the pivot and is determined by the particular material used to print the pantographic structure considered. This expression allows to properly describe the deformation features of pantographic structures. In fact, it contains terms accounting for elongation and bending deformations, which are weighted by the

rigidities $\mathbb{K}_e$ and $\mathbb{K}_b$, and for the macroscopic shear deformation (at a microscopic level the shear deformation is related to the torsion of the interconnecting pivots), with stiffness $\mathbb{K}_p$. The variational formulation allows to derive all the mechanical properties by means of minimization of the energy. In [20] first experimental evidences and numerical simulations have been presented. The pantographic structures there considered were polyamide printed structures. Here we present results relative to metallic printed structures. The central point of this work is to show how the mechanical properties of this particular structure do not depend on the material itself (clearly the parameters $\mathbb{K}_i$ to be used in the model depend on it, but they define only the range limits of the forces involved), but only on the geometry of the system: in this sense the pantographic structures constitute a class of metamaterials. The homogenization procedure defined in [8] is so well founded that the second gradient macro-model can be used to produce results, through numerical simulations compared to experimental data, even in the case of pantographic structures where the distance between the pivots (theoretically, the smaller this distance, the more the structure can be assimilated to a continuous) is quite large. Consider, for example, the different structures shown in Fig. 2, all of which can be described using energy in Eq. (1), even for the case (a), an example of a wide-knit pantographic structure. This aspect of the homogenization procedure for pantographic metamaterial is currently being studied.

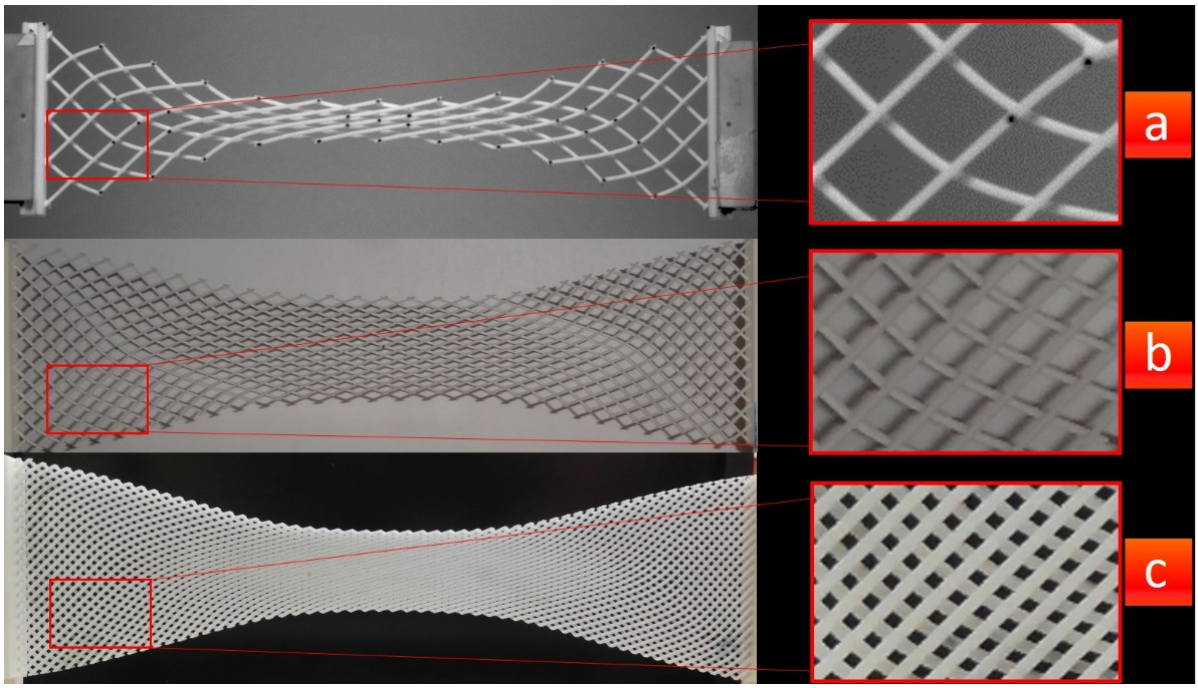

Fig. 2. A wide-knit pantographic structure (a) and two structures with a thicker mesh (b,c)

The simplest experimental test that can be performed on pantographic structures is known as the BIAS extension test [20] (it is specifically called the BIAS extension and not just the extension, because it is performed in a biased direction with respect to the direction of the fibers).

This particular test is performed by tightening the short sides of the pantograph structure to observe the effects of the second gradient. In fact, as we can see in Fig. 3, if the short sides are not blocked, then, in theory, we should measure a zero strain energy, because of the truss effect: up to the point where all the fibers become parallel the extension energy is zero (or negligible). If the short sides are not tightened, the bending energy (second gradient, as it can be seen in Eq. (1) where the second gradients of the placement appear only in the bending term) is also cancelled out. Therefore, this test was designed in the field of pantographic

structures specifically to observe the second gradient effect. Some experimental results are presented and compared with numerical simulations in the next section.

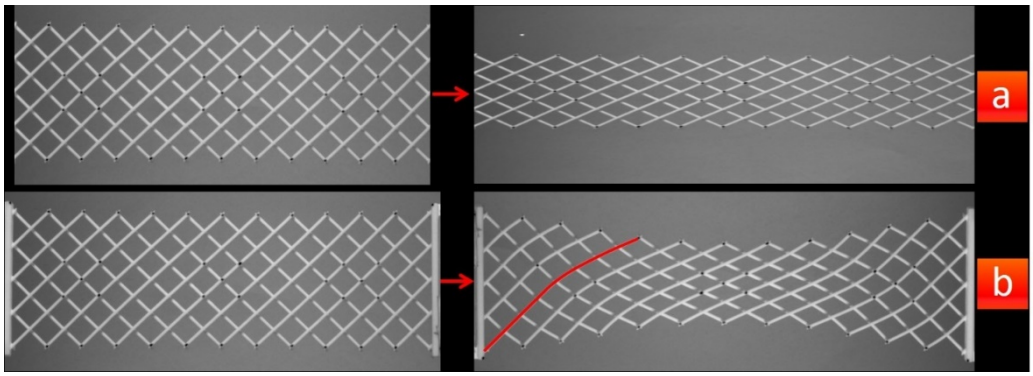

Fig. 3. Examples of BIAS extension tests without clamping (a) and with clamping of the short sides (b). In case (b) the bending of the fibres is theoretically described by a second gradient term in the deformation energy

3 Comparison between experimental measurements and numerical simulations

In this section we present the experimental measurements for two (theoretically) identical steel molded samples, namely "Sample A" and "Sample B". There is a fundamental difference between the two samples: the second, sample B, suffered a fracture in the first stage of deformation and therefore the total amount of force exerted in the BIAS test is lower than that obtained for sample A (see Fig. 4). The samples are molded in 316L stainless steel. Both specimens have a rectangular shape with dimensions of $30\ mm \times 90\ mm$.

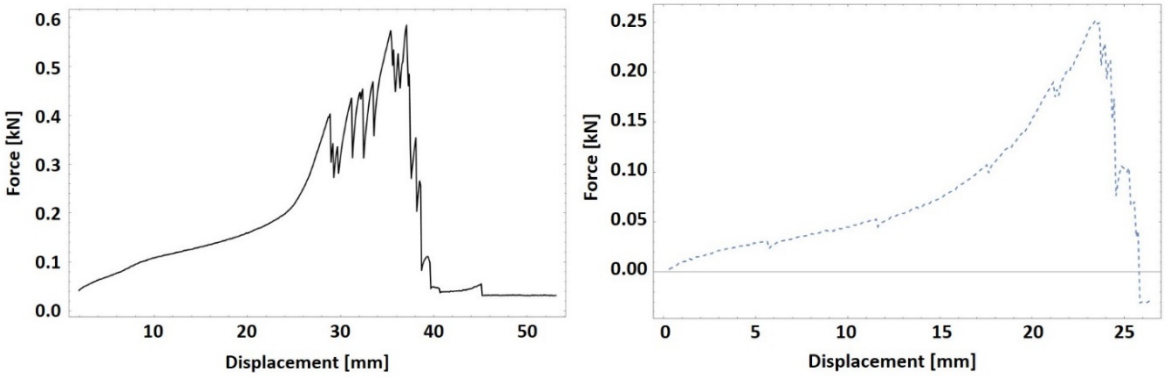

Fig. 4. Force-displacement plots for two steel (theoretically) identical pantographic structures. One of the two (right plot, the pantographic structure we referred to as Sample B) has joined the fracture in a very early stage of deformation, probably for some random differences produced during the stage of manufacturing

First of all, we want to underline that the general shape of the force-displacement curve is the same in the case of Samples A and B and it is only necessary to change the scale of values. But if it is simply understandable in the case of two samples printed in the same material, it is surprising to find a very similar curve also in the case of samples printed in polyamide [9] or aluminum [21] (again, the only thing that changes is the range of the force in question). The behavior measured in the BIAS experiments also shows that the tolerance to damage to pantographic structures is noteworthy. This aspect is included in the force-displacement diagrams in Fig. 4. The force-displacement diagram for pantographic fabrics usually shows a peak at the end of the stiffening phase. After the peak, the structure

undergoes a sequential rupture of its sub-components, typically the cutting of the pivots, resulting in avalanche softening. The gradual softening leading to failure suggests that the topology of the structure and the deformability properties of its members are such that, when a breakage of the subcomponent occurs, the load can be redistributed into an attenuating agent that prevents simultaneous catastrophic failures. In fact, this tolerance to damage is also shown by the pantographic structure when the failure of its sub-components occurs before the peak load.

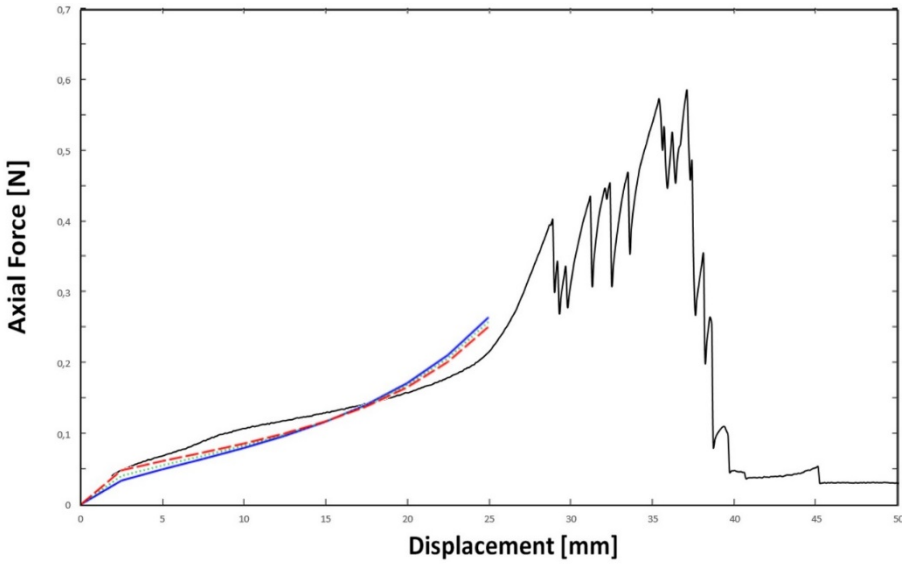

Fig. 5. Qualitative comparison between experimental data (Sample B) and numerical simulations for different values of the γ exponent: $\gamma = 1.2$ (red dashed), $\gamma = 1.3$ (green dotted) and $\gamma = 1.4$ (blue). A more accurate analysis can be conducted to obtain results closer to the experimental data

Figure 5 shows the comparison between numerical simulations of the force-displacement graph and the experimental data. The numerical simulations are obtained for different values of the γ exponent. Further, more accurate analyses can be carried out to obtain simulations more in line with the data. For example, it must be considered that the constituent parameters of objects obtained by additive manufacturing are not the same as the original material (Young's modulus of pantographic structures printed in 316L stainless steel is clearly lower than that of metal [22]). For this reason, it would be appropriate to carry out precise studies to identify the real constituent parameters in order to obtain more adherent simulations.

Figure 6 shows the comparison between the deformed shapes of specimen B obtained by numerical simulations and the experimental measurements (for Sample A, it is actually not possible to make similar comparisons in case of early rupture, but see [21] for a proposed approach in this direction). The numerical simulation, in which we minimize the continuous energy derived in Eq. (1), was performed for different values of the imposed displacement. We first identified the parameters $\mathbb{K}_e$, $\mathbb{K}_b$, and $\mathbb{K}_p$ with a procedure similar to that described in [23-25] and in a second phase we compared the calculated force-displacement curve and the deformed shapes of the pantographic structure with the experimental data to obtain a better estimate of the constituent parameters.

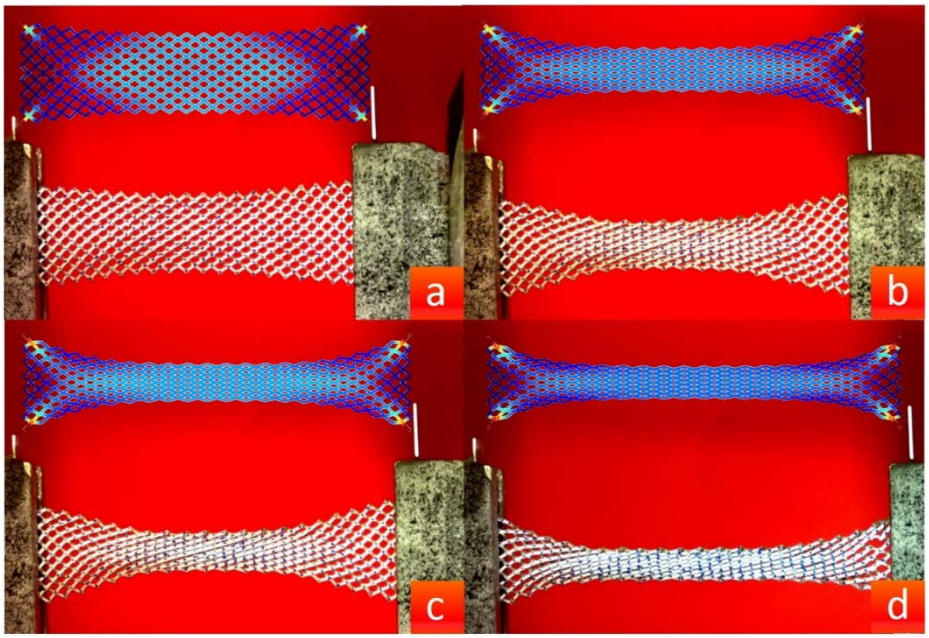

Fig. 6. Comparison between experiments performed on Sample A and numerical simulations for different values of imposed displacement: (a) 1 mm; (b) 22 mm; (c) 26 mm; (d) 35 mm. In (d) one can see that the structure has already undergone the failure stage. In color scale the total deformation energy is plotted

4 Conclusion

In this article we presented an example of a new class of metamaterials, the pantographic structures. The BIAS extension test carried out on two stainless steel molded samples has been studied from both an experimental and a numerical point of view.

An interesting perspective of this work consists in the study and analysis of damage in pantographic structures, in order to obtain estimates of experimental data such as those shown in Fig. 7. This type of study has already been started and useful references can be found in [26-34].

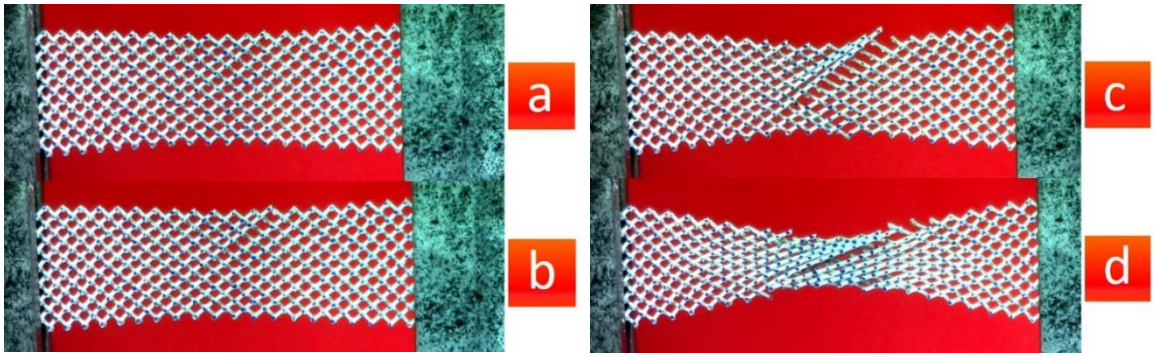

Fig. 7. Emerging of fracture in Sample B. In (b) it is already visible the arising of fracture: a whole fiber has lost the connections (pivots) with the fibers of the other family

A possible generalization of the pantographic structure presented in this work is the study of pantographic structures embedded in soft matrices. Useful results in this framework can be found in [35-38] and [39] for engineering relevant composites.

Numerical tools are increasingly important in the study of metamaterials. A powerful numerical method for solving minimum problems, such as the one described qualitatively in

this article, is represented by isogeometric analysis. Results relevant to the study of pantographic structures can be found in [40-45].

Acknowledgments. *This work was supported by a grant from the Government of the Russian Federation (contract No. 14.Y26.31.0031).*

References

[1] Pideri C, Seppecher P. A second gradient material resulting from the homogenization of an heterogeneous linear elastic medium. *Continuum Mechanics and Thermodynamics*. 1997;9(5): 241-257.
[2] Dell'Isola F, Seppecher P. The relationship between edge contact forces, double forces and interstitial working allowed by the principle of virtual power. *Comptes rendus de l'Académie des sciences. Série IIb, Mécanique, physique, astronomie*. 1995;7: 43-48.
[3] Abali BE. *Computational Reality*. Singapor: Springer; 2016.
[4] Abali BE, Müller WH, Dell'Isola F. Theory and computation of higher gradient elasticity theories based on action principles. *Archive of Applied Mechanics*. 2017;87(9): 1495-1510.
[5] Forest S, Sab K. Stress gradient continuum theory. *Mechanics Research Communications*. 2012;40: 16-25.
[6] Alibert JJ, Seppecher P, Dell'Isola F. Truss modular beams with deformation energy depending on higher displacement gradients. *Mathematics and Mechanics of Solids*. 2003;8(1): 51-73.
[7] Seppecher P, Alibert JJ, Dell'Isola F. Linear elastic trusses leading to continua with exotic mechanical interactions. *Journal of Physics: Conference Series*. 2011;319(1); 012018
[8] Dell'Isola F, Giorgio I, Pawlikowski M, Rizzi NL. Large deformations of planar extensible beams and pantographic lattices: heuristic homogenization, experimental and numerical examples of equilibrium. *Proc. R. Soc. A*. 2016;472(2185): 20150790.
[9] Dell'Isola F, Lekszycki T, Pawlikowski M, Grygoruk R, Greco L. Designing a light fabric metamaterial being highly macroscopically tough under directional extension: first experimental evidence. *Zeitschrift für angewandte Mathematik und Physik*. 2015;66(6): 3473-3498.
[10] Rahali Y, Giorgio I, Ganghoffer JF, Dell'Isola F. Homogenization à la Piola produces second gradient continuum models for linear pantographic lattices. *International Journal of Engineering Science*. 2015;97: 148-172.
[11] Alibert JJ, Della Corte A. Second-gradient continua as homogenized limit of pantographic microstructured plates: a rigorous proof. *Zeitschrift für angewandte Mathematik und Physik*. 2015;66(5): 2855-2870.
[12] Alibert JJ, Della Corte A, Giorgio I, Battista A. Extensional Elastica in large deformation as Γ-limit of a discrete 1D mechanical system. *Zeitschrift für angewandte Mathematik und Physik*. 2017;68(2): 42.
[13] Germain P. La méthode des puissances virtuelles en mécanique des milieux continus. Première partie: théorie du second gradient. *J. Mécanique*. 1973;12: 236-274.
[14] Germain P. The method of virtual power in continuum mechanics. Part 2: Microstructure. *SIAM Journal on Applied Mathematics*. 1973;25(3): 556-575.
[15] Mindlin RD. Micro-structure in linear elasticity. *Archive for Rational Mechanics and Analysis*. 1964;16(1): 51-78.
[16] Mindlin RD. Second gradient of strain and surface-tension in linear elasticity. *International Journal of Solids and Structures*. 1965;1(4): 417-438.
[17] Mindlin RD, Eshel N. On first strain-gradient theories in linear elasticity. *International Journal of Solids and Structures*. 1968;4(1):109-124.

[18] Toupin RA. Theories of elasticity with couple-stress. *Archive for Rational Mechanics and Analysis*. 1964;17(2): 85-112.
[19] Sedov L. Variational methods of constructing models of continuous media. In: *Irreversible aspects of continuum mechanics and transfer of physical characteristics in moving fluids*. Springer; 1968. p.346-358.
[20] Dell'Isola F, Cuomo M, Greco L, Della Corte A. Bias extension test for pantographic sheets: numerical simulations based on second gradient shear energies. *Journal of Engineering Mathematics*. 2017;103(1): 127-157.
[21] Spagnuolo M, Barcz K, Pfaff A, Dell'Isola F, Franciosi P. Qualitative pivot damage analysis in aluminum printed pantographic sheets: Numerics and experiments. *Mechanics Research Communications*. 2017;83: 47-52.
[22] Čapek J, Machova M, Fousova M, Kubásek J, Vojtěch D, Fojt J, Yablonska E, Lipov J, Ruml T. Highly porous, low elastic modulus 316L stainless steel scaffold prepared by selective laser melting. *Materials Science and Engineering: C*. 2016;69: 631-639.
[23] Placidi L, Andreaus U, Giorgio I. Identification of two-dimensional pantographic structure via a linear D4 orthotropic second gradient elastic model. *Journal of Engineering Mathematics*. 2017;103(1): 1-21.
[24] Placidi L, Barchiesi E, Della Corte A. Identification of two-dimensional pantographic structures with a linear D4 orthotropic second gradient elastic model accounting for external bulk double forces. In: *Mathematical Modelling in Solid Mechanics*. Singapore: Springer; 2017. p.211-232.
[25] De Angelo M, Barchiesi E, Giorgio I, Abali BE. Numerical identification of constitutive parameters in reduced-order bi-dimensional models for pantographic structures: application to out-of-plane buckling. *Archive of Applied Mechanics*. 2019;89(7): 1-26.
[26] Placidi L, Barchiesi E. Energy approach to brittle fracture in strain-gradient modelling. *Proc. R. Soc. A.* 2018;474(2210): 20170878.
[27] Placidi L, Misra A, Barchiesi E. Two-dimensional strain gradient damage modeling: a variational approach. *Zeitschrift für angewandte Mathematik und Physik*. 2018;69: 56.
[28] Barchiesi E, Ganzosch G, Liebold C, Placidi L, Grygoruk R, Müller WH. Out-of-plane buckling of pantographic fabrics in displacement-controlled shear tests: experimental results and model validation. *Continuum Mechanics and Thermodynamics*. 2019;31(1): 33-45.
[29] Placidi L, Barchiesi E, Misra A, Andreaus U. Variational methods in continuum damage and fracture mechanics. In: Altenbach H, Öchsner A. (eds.) *Encyclopedia of Continuum Mechanics*. Springer: 2018.
[30] Placidi L, Misra A, Barchiesi E. Simulation results for damage with evolving microstructure and growing strain gradient moduli. *Continuum Mechanics and Thermodynamics*. 2018: 1-21.
[31] Contrafatto L, Cuomo M. A new thermodynamically consistent continuum model for hardening plasticity coupled with damage. *International journal of solids and structures*. 2002;39(25): 6241-6271.
[32] Contrafatto L, Cuomo M. A framework of elastic–plastic damaging model for concrete under multiaxial stress states. *International Journal of Plasticity*. 2006;22(12): 2272-2300.
[33] Cuomo M, Contrafatto L, Greco L. A variational model based on isogeometric interpolation for the analysis of cracked bodies. *International Journal of Engineering Science*. 2014;80: 173-188.
[34] Cuomo M. Continuum damage model for strain gradient materials with applications to 1D examples. *Continuum Mechanics and Thermodynamics*. 2019;24(8): 2374-2391.
[35] Franciosi P, Spagnuolo M, Salman OU. Mean Green operators of deformable fiber networks embedded in a compliant matrix and property estimates. *Continuum Mechanics and Thermodynamics*. 2019;31(1): 101-132.

[36] Franciosi PA. Decomposition method for obtaining global mean Green operators of inclusions patterns. Application to parallel infinite beams in at least transversally isotropic media. *International Journal of Solids and Structures*. 2018;147: 1-19.
[37] Franciosi P, Lormand G. Using the radon transform to solve inclusion problems in elasticity. *International Journal of Solids and Structures*. 2004;41(3-4): 585-606.
[38] Franciosi P, Brenner R, El Omri A. Effective property estimates for heterogeneous materials with cocontinuous phases. *Journal of Mechanics of Materials and Structures*. 2011;6(5): 729-763.
[39] Rosati L, Marmo F, Serpieri R. Enhanced solution strategies for the ultimate strength analysis of composite steel-concrete sections subject to axial force and biaxial bending. *Computer methods in applied mechanics and engineering*. 2008;197(9-12): 1033-1055.
[40] Greco L, Cuomo M. An implicit G1 multi patch B-spline interpolation for Kirchhoff–Love space rod. *Computer Methods in Applied Mechanics and Engineering*. 2014;269: 173-197.
[41] Greco L, Cuomo M. B-Spline interpolation of Kirchhoff-Love space rods. *Computer Methods in Applied Mechanics and Engineering*. 2013;256: 251-269.
[42] Greco L, Cuomo M. An isogeometric implicit G1 mixed finite element for Kirchhoff space rods. *Computer Methods in Applied Mechanics and Engineering*. 2016;298: 325-349.
[43] Cazzani A, Malagù M, Turco E. Isogeometric analysis of plane-curved beams. Mathematics and Mechanics of Solids. 2016;21(5): 562-577.
[44] Cazzani A, Malagù M, Turco E, Stochino F. Constitutive models for strongly curved beams in the frame of isogeometric analysis. *Mathematics and Mechanics of Solids*. 2016;21(2): 182-209.
[45] Cazzani A, Malagù M, Turco E. Isogeometric analysis: a powerful numerical tool for the elastic analysis of historical masonry arches. *Continuum Mechanics and thermodynamics*. 2016;28(1-2): 139-156.